ELSEVIER

Available online at www.sciencedirect.com

SciVerse ScienceDirect

Energy Procedia 16 (2012) 1072 – 1077

Energy Procedia

2012 International Conference on Future Energy, Environment, and Materials

Numerical Simulation of Gas and Liquid Flow within a Vortex Spray Tower

Leilei Li, Bingtao Zhao*

School of Energy and Power Engineering, University of Shanghai for Science and Technology, 516 Jungong Road, Shanghai 200093, China

Abstract

The vortex spray tower is widely used by researchers because the cyclonic flow can be generated which promote the relative flow between the gas and liquid phases. In this work, the CFD software is used to numerically simulate the flow field in the vortex spray tower. The figures of tangential velocity, axial velocity, radial velocity and particle tracks are provided, and the discipline of the gas and liquid flow in the vortex spray tower is analyzed.

Keywords: vortex spray tower；cyclonic flow ;CFD; numerically simulate ;tangential velocity;particle tracks

1. Introduction

Spray tower is widely used in the air pollution control field such as desulfuration, denitrification and CO2 removing. With the advantages of high relative velocity of the gas and liquid, large contacted area and simple device structure [1,2], spray tower has become one of the most important gas pollutants removal devices which are preferably utilized in the field of both science and engineering. Recently, Computational Fluid Dynamics (CFD) technique has been more and more prevalent to simulate the chemical absorption process and result. It has the advantages of low cost, fast design and calculate, complete information and strong simulation analog capability [3-5].

Based on the structure of the spray tower, the tangential gas admission is utilized to generate cyclonic flow in the vortex spray tower. In this case, the contact of gas and liquid is more complete, the mass

* Corresponding author. Tel.: +86-21-55272740; fax:+86-21-55273704.
E-mail address: zhaobingtao@usst.edu.cn (B. Zhao).

 doi:10.1016/j.egypro.2012.01.171

transfer is stronger, and the relative gas-liquid velocity and the absorption efficiency are higher. Therefore, the vortex spray tower is accepted and studied by more and more domestic and foreign researchers. Javed et al [6,7] had investigated the mass transfer and CO2 absorption performance in the vortex spray tower by doing experiments, and proved the enhancement effect of cyclonic flow on mass transfer and CO2 absorption performance. However, the further research of vortex spray tower has not been proposed, so it is necessary to study more complicated situation of the vortex spray tower. Many researchers had done the numerical simulation of the flow field and particle tracks of the cyclone separator and spray tower which provided very good models for the research of the vortex spray tower [8-12].

In this paper, the author did the numerical simulation of the flow field of the vortex spray tower, provided the figures of tangential velocity, axial velocity, radial velocity and particle tracks, and analyzed the discipline of the gas and liquid flow in the vortex spray tower.

2. Model and approach

2.1. Physical model and grid system

Fig. 1 and 2 show the schematic diagram and the grid of the vortex spray tower. Considered the practical application and the size of the tower, the hexahedral structured grid is used to divide the model. It contains 18600 control cells, 57520 faces and 20421 nodes.

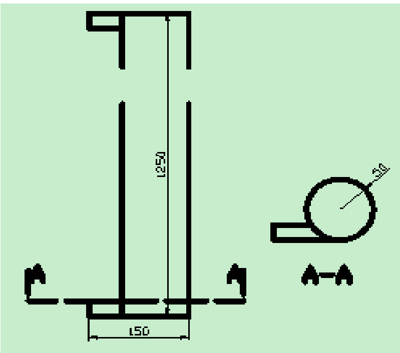

Fig.1. Schematic diagram of the vortex spray tower

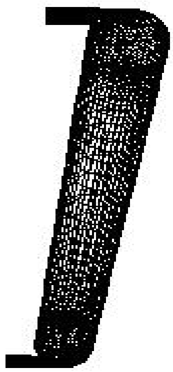

Fig.2. Grid of the vortex spray tower

2.2. Governing equations

Usually, Fluid flows have been mathematically described by a set of nonlinear and partial differential equations named the Navier-Stokes equation. For the steady and incompressible fluid flow in cyclones, a Reynolds-averaged Navier-Stokes equations (RANS) can be expressed as:

$$\rho u_j \frac{\partial u_i}{\partial x_j} = -\frac{\partial p}{\partial x_i} + \frac{\partial}{\partial x_j}\left[\mu\left(\frac{\partial u_i}{\partial x_j} + \frac{\partial u_j}{\partial x_i}\right)\right] + \frac{\partial \tau_{ij}}{\partial x_j} \quad (1)$$

$$\frac{\partial u_i}{\partial x_i} = 0 \quad (2)$$

Where the superscripts i, j= 1,2,3 indicate the components in the Cartesian coordinate system u , ρ, p and μ represent the fluid velocity, density, pressure and viscosity, respectively, and

$$\tau_{ij} = -\rho\overline{u_i'u_j'} \tag{3}$$

is defined as the Reynolds stress tensor which represents the effects of the turbulent fluctuations on the fluid flow. The dash represents the fluctuating part and the over bar represents a Reynolds average. However, the above equations are not closed unless the Reynolds stress tensor is determined by use of the turbulence model. In order to modeling the Reynolds stress tensor, many turbulence models have been developed to utilize the cyclone simulation. The representative models include the k-ε Model (KEM), Algebraic Stress Model (ASM) and Reynolds Stress Model (RSM). In these models, The RSM presents the characteristics of anisotropic turbulence and requires the solution of transport equations for each of the Reynolds stress components as well as for dissipation transport. Therefore, this model provides a potentially excessive computational effort for the three-dimensional simulation of the fluid flow in cyclone. According to assumptions of governing equations, the transport equation of RSM is simply written as:

$$\frac{\partial}{\partial x_k}\left(\rho u_k \overline{u_i'u_j'}\right) = -\frac{\partial}{\partial x_k}\left(\frac{\mu_t}{\sigma_k}\frac{\partial \overline{u_i'u_j'}}{\partial x_k}\right) - \rho\left(\overline{u_i'u_k'}\frac{\partial u_j}{\partial x_k} + \overline{u_j'u_k'}\frac{\partial u_i}{\partial x_k}\right) + \overline{p\left(\frac{\partial u_i'}{\partial x_j} + \frac{\partial u_j'}{\partial x_i}\right)} - 2\mu\overline{\frac{\partial u_i'}{\partial x_k}\frac{\partial u_j'}{\partial x_k}} \tag{4}$$

Where the eddy viscosity μ is determined by the usual formula:

$$\mu_t = \rho C_\mu \frac{k^2}{\varepsilon} \tag{5}$$

The turbulent kinetic energy k and the turbulent dissipation rate ε are solved by the following equations, respectively:

$$\frac{\partial}{\partial t}(\rho k) + \frac{\partial}{\partial x_i}(\rho k u_i) = \frac{\partial}{\partial x_j}\left[\left(\mu + \frac{\mu_t}{\sigma_k}\right)\frac{\partial k}{\partial x_j}\right] + \frac{1}{2}\left(P_{ii} + G_{ii}\right) - \rho\varepsilon\left(1 + 2M_t^2\right) \tag{6}$$

$$\frac{\partial}{\partial t}(\rho \varepsilon) + \frac{\partial}{\partial x_i}(\rho \varepsilon u_i) = \frac{\partial}{\partial x_j}\left[\left(\mu + \frac{\mu_t}{\sigma_\varepsilon}\right)\frac{\partial \varepsilon}{\partial x_j}\right] + C_{\varepsilon 1}\frac{1}{2}\left[P_{ii} + C_{\varepsilon 3}G_{ii}\right]\frac{\varepsilon}{k} - C_{\varepsilon 2}\rho\frac{\varepsilon^2}{k} \tag{7}$$

The values of the constants which appear in the RSM model are usually assigned as follows: σ_k =0.82, C_μ=0.09, σ_ε =1.0, $C_{\varepsilon 1}$=1.44, and $C_{\varepsilon 2}$ =1.92.

2.3. Solution strategy

For the gas phase, the RNG k- ε and Reynolds Stress turbulent models are employed to solve the governing equations. And the second order upwind and QUICK schemes are respectively selected to use. The SIMPLE algorithm is applied for pressure-velocity coupling and PRESTO for the pressure discretization. For the liquid phase, the FLUENT software provided several Multiphase models. When the concentration of particle is high, the multiphase models can be used. However, if the volume fraction of the particle is lower than 10%, the Discrete Phase Model (DPM) is usually selected. In this work, the DPM is employed with the Discrete Random walk model to track the orbit of the particles.

2.4. Boundary conditions

(1) Boundary condition at the inlet. The air at the room temperature is employed, which ρ=1.225kg/m^3. The type is velocity inlet with the hydraulic diameter 18mm, and the turbulence intensity can obtain by:

$$I=0.16\,(Re)\,-1/8 \tag{8}$$

(2) Boundary condition at the outlet. The type is set as outflow.

(3)A non-slip boundary condition is imposed on the wall. Generally, the log-law of the standard wall function is used for the wall treatment as following:

$$u^+ = \begin{cases} \frac{1}{\kappa}\ln\left(Ey^+\right) & y^+ > 11.225 \\ u^+ & y^+ < 11.225 \end{cases} \tag{9}$$

and near the wall, the value of the dissipation rate of the turbulent kinetic energy is given by

$$\varepsilon = \frac{C_\mu^{3/4} k^{3/2}}{\kappa y} \tag{10}$$

where κ=0.4187 (von Karmon constant), E=9.793.

For the liquid phase, the injection type is solid-cone, both the boundary conditions at the inlet and outlet are escape, which is wall-film at the wall.

3. Results

3.1. Tangential velocity

Fig 3 and 4 display the tangential velocity with different flowrate at z=0.6m and the tangential velocity with different height at Q=200L/min. It is observed that, the tangential velocity, as a function of position, is increasing with an increasing radius in the domain flow region and tends to zero from the boundary layer to the wall. It should be noted that the distribution of tangential velocity in the cyclone spray scrubber is significantly different from that in the conventional reverse-flow cyclone separator, which is called “Rankine vortex”. This phoneme is consistent with the experimental result reported in literature [13]. In addition, with the increase of flowrate, the tangential velocity increases at the same monitoring section, indicating increasing flowrate gives rise to the increase of swirl intensity. In the same flowrate, the tangential velocity reduces with the increasing height of cyclone spray scrubber, indicating the swirl flow is gradually decayed by the wall friction. But high flowrate or inlet velocity is helpful to prolong the decaying distance of swirl flow. Moreover, due to the instability of vortex, the tangential velocity dos not present strictly an axisymmetric distribution at the different height.

3.2. Axial velocity

Fig 5 and 6 display the axial velocity with different flowrate at z=0.6m and the axial velocity with different height at Q=200L/min. It is observed that, in the central region, the axial velocity is negative, which indicates that there is downward flow in this region. Both the downward axial velocity in the central region and upward axial velocity in the outer region increase with the increase of flowrate. Moreover, in the same flowrate, the axial velocity value reduces with the increase of height, indicating the velocity gradient is reduced accordingly. This may be attributed to the decay of the swirl flow.

Additionally, the axial velocity presents the strong non-symmetry and instability in the z direction, which is similar to the tangential velocity.

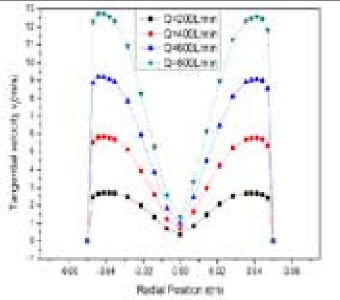

Fig.3. tangential velocity with different flowrate at z=0.6m

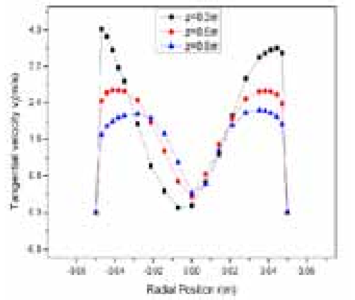

Fig.4. tangential velocity with different height at Q=200L/min

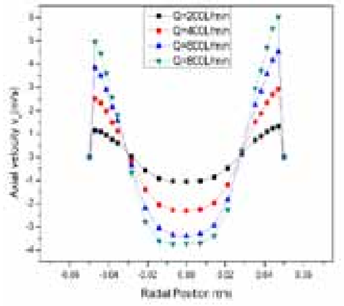

Fig.5. axial velocity with different flowrate at z=0.6m

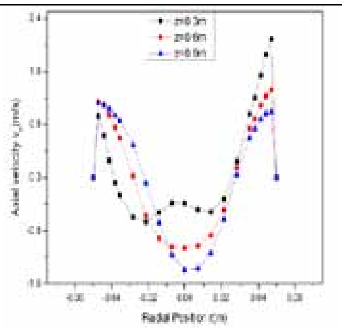

Fig.6. axial velocity with different height at Q=200L/min

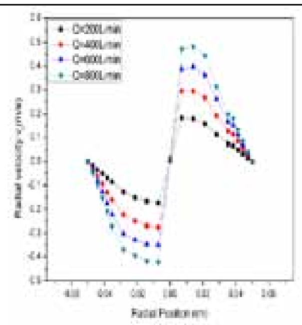

Fig.7. radial velocity with different flowrate at z=0.6m

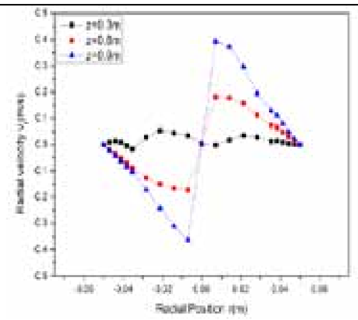

Fig.8. radial velocity with different height at Q=200L/min

3.3. Radial velocity

Fig 7 and 8 show the radial velocity with different flowrate at z=0.6m and the radial velocity with different height at Q=200L/min. It is found that the radial velocity is far lower than the tangential velocity, and increases with the increasing flowrate. Further, the radial velocity increases with the increase of height. And the radial velocity is not strictly point symmetric.

3.4. Particle Tracks

The water is used to simulate the liquid flow in the vortex spray tower. Its flow rate is 3L/min, the initial droplet size is 133.8μm and initial droplet velocity is 3.7m/s. Fig.9 shows the particle tracks in the vortex spray tower. The particles are sprayed from the nozzle at the top of the tower, and generated liquid film in the wall.

Fig.9. Liquid particle tracks of the vortex spray tower

Acknowledgements

This work was jointly sponsored by Shanghai Natural Science Foundation (No. 08ZR1415100) and National Natural Science Foundation of China (No.50806049).

References

[1] Liu GR, Wang ZW, Wei YL, Ji QL. The model and experimental study of desulphurization of flue gas in the spray tower. *J Chem Ind* 2010;61:2462-67.

[2] Tan ZC. An analytical model for the fractional efficiency of a uniflow cyclone with a tangential inlet. *Powder Technol* 2008;183:147-151.

[3] Wang FJ. The principle and application of the CFD software. Tsinghua University Press. 2004.

[4] Wen Z, Shi LC, Ren YR. The application course of the hydraulic calculation. Tsinghua University Press. 2009.

[5] Jing F, Huang P. Advanced application and example analysis of FLUENT. Tsinghua University Press. 2008.

[6] Javed KH, Mahmud T, Purba E. The CO2 capture performance of a high-intensity vortex spray scrubber. *Chem Eng J*. 2010;162:448-456.

[7] Javed KH, Mahmud T, Purba E. Enhancement of mass transfer in a spray tower using swirling gas flow. *Chem Eng Research Design*. 2006;84:465-477.

[8] Su YX, Zhao BT, Zheng AQ. Simulation of turbulent flow in square cyclone separator with different gas exhaust. *Ind Eng Chem Research*. 2011;50:12162-12169.

[9] Zhao HQ, Jiang HH, Xie WZ. The numerical simulation research of the flow field in the cyclone separator based on LES. *J Environ Eng*. 2009;3:758-763.

[10] Lin T, Ahmadi G. Particle deposition in turbulent duct flows-comparisons of different model prediction. *J Aerosol Science*. 2007;38:377-397.

[11] Hao JM, Ma GD. Air pollustion control engineering. Higher Education Press. 2002.

[12] Zhang CH, Li LT, Duan RZ, Liu LS. The numerical simulation of the an swirl flow and spray process in the columnar combustion chamber. *J HB Ind University*. 2010;39:82-89.

[13] Shen, H.G., Yin X.X., Huang, S.F. and Zhao B.T., 2002, Experimental study on swirl flow in circular pipe using a multi-hole probe, Proceeding of national HVAC (In Chinese), 2002.